between Zr and Li atoms is rather too long to have any significant interactions between them. The eclipsed conformation of the C_{cage}–$SiMe_3$ groups of the opposing ligands in I could be due to the presence of a $Li^+(THF)_2$ moiety.

In addition to the X-ray analysis, compound I was also characterized by ^1H, ^{11}B, and ^{13}C NMR and IR spectroscopy.[8] Although the ^1H and ^{13}C NMR spectra indicated the presence of two nonequivalent $SiMe_3$ groups and two nonequivalent THF molecules, the proton-coupled ^{11}B NMR spectrum of I showed broad, ill-defined resonances at 33.16, 25.48, and −16.32 ppm, whose relative areas indicate a 1:2:1 distribution of basal and apical BH groups, respectively. This indicates that I could be either a closo or a commo complex, thus inferring that the ^{11}B NMR spectroscopy is not an effective tool to elucidate the structure of I. The presence of the coordinated THF and the heterocarborane complex was also confirmed by the IR spectrum of I.[8]

The bright yellow color of I may be due to the presence of a $[Li(THF)_2]^+$ moiety. The bent structure of the complex could be rationalized on the basis of the location of the THF molecule and the Cl atom on the *commo*-Zr metal. Similar bent-sandwich geometries have been recently reported for anionic carborane complexes, $[U(C_2B_9H_{11})_2Cl_2]^{2-}$ and $[3,3'\text{-}(THF)_2\text{-}commo\text{-}3,3'\text{-}Sm(3,1,2\text{-}SmC_2B_9H_{11})_2]^-$.[9,10] It is important to note that the coordination of a Lewis base to the apical heteroatom of the main group results in slip distortion of the heterocarborane cage, invariably toward the boron atoms above the C_2B_3 face.[11] However, the bond distances in I indicate that the *commo*-Zr metal is symmetrically bonded to the carborane cages, and hence, the bonding of a THF molecule to the zirconium metal in the complex has very little effect on the cage geometries unlike the cases of main-group metallacarboranes. In any case, compound I represents the first Zr^{IV} sandwich carborane complex ever to be reported.

The presence of a chlorine atom on zirconium metal suggests that I could be converted to a neutral alkyl derivative of the type $R\text{–}Zr[\eta^5\text{-}(SiMe_3)_2C_2B_4H_4]_2Li(THF)_2$ since its most exciting prospects lie in the potential for developing better catalysts than those based on the mixture of zirconocene alkyl derivative and methylaluminoxane in the Ziegler–Natta olefin polymerization systems. Such a neutral, isoelectronic, carborane-based analogue obviates the severe problems of devising an innocent, noncoordinating counteranion which have plagued the zirconocene system.[1] Our efforts in such an endeavor are currently in progress.

Acknowledgment. This work was supported by grants from the National Science Foundation (CHE-8800328), the Robert A. Welch Foundation (N-1016), and the donors of the Petroleum Research Fund, administered by the American Chemical Society. Dr Siriwardane thanks the State of Louisiana (Grant No. NSF-LaSER (1990)-RFAP-07) and the Louisiana Tech University for a faculty development and summer research stipend to conduct research at Southern Methodist University.

Supplementary Material Available: Tables of positional and thermal parameters, bond distances, bond angles, and torsion angles for compound I (8 pages); listing of observed and calculated structure factors for compound I (18 pages). Ordering information is given on any current masthead page.

(8) Spectroscopic data for I: ^1H NMR (C_6D_6, relative to external Me_4Si) δ 3.82 (s, 4 H, THF), 3.6 [br, ill-defined peak, 6 H, basal H_t, $^1J(^1H\text{–}^{11}B)$ = unresolved], 3.35 (s, 8 H, THF), 2.6 [br, ill-defined peak, 2 H, apical H_t, $^1J(^1H\text{–}^{11}B)$ = unresolved], 1.15 (s, 4 H, THF), 1.09 (s, 8 H, THF), 0.30 (s, 18 H, $SiMe_3$), 0.21 (s, 18 H, $SiMe_3$); ^{11}B NMR (C_6D_6, relative to external $BF_3\cdot OEt_2$) δ 33.16 [br, ill-defined peak, 1 B, basal BH, $^1J(^{11}B\text{–}^1H)$ = unresolved], 25.48 [br, ill-defined peak, 2 B, basal BH, $^1J(^{11}B\text{–}^1H)$ = unresolved], −16.32 [br, ill-defined peak, 1 B, apical BH, $^1J(^{11}B\text{–}^1H)$ = unresolved]; ^{13}C NMR (relative to external Me_4Si) δ 123.92 [s (br), cage carbons (SiCB)], 123.42 [s (br), cage carbons (SiCB)], 76.43 [t, 2 C, Zr–THF, $^1J(^{13}C\text{–}^1H)$ = 150 Hz], 68.63 [t, 4 C, Li–THF, $^1J(^{13}C\text{–}^1H)$ = 148 Hz], 33.24 [t, 2 C, Zr–THF, $^1J(^{13}C\text{–}^1H)$ = 127 Hz], 25.49 [t, 4 C, Li–THF, $^1J(^{13}C\text{–}^1H)$ = 134 Hz], 3.65 [q, $SiMe_3$, $^1J(^{13}C\text{–}^1H)$ = 119.8 Hz], 3.25 [q, $SiMe_3$, $^1J(^{13}C\text{–}^1H)$ = 118.81 Hz]; IR (cm^{-1}; C_6D_6 vs C_6D_6) 2954 (vs), 2896 (vs) [ν(C–H)], 2543 (vvs), 2496 (vs, sh), 2449 (m, sh) [ν(B–H)], 1443 (w), 1402 (w, br) [$\delta\text{-}(CH)_{asym}$], 1355 (w, br), 1337 (w), 1249 (vs) [$\delta(CH)_{sym}$], 1179 (m, s), 1126 (w, br), 1067 (w, sh), 1044 (m), 1002 (m, br), 914 (w, sh), 844 (vvs, br) [ρ(CH)], 761 (s, s), 703 (w, br), 632 (m, s) [ν(Zr–Cl)], 602 (w, sh), 532 (w, br), 479 (w, br).

(9) Fronczek, F. R.; Halstead, G. W.; Raymond, K. N. *J. Am. Chem. Soc.* **1977**, *99*, 1769.
(10) Manning, M. J.; Knobler, C. B.; Hawthorne, M. F. *J. Am. Chem. Soc.* **1988**, *110*, 4458.
(11) Hosmane, N. S.; Maguire, J. A. *Adv. Organomet. Chem.* **1990**, *30*, 99.

New Nuclear Magnetic Resonance Technique for Determining Long-Range Heteronuclear $^1H\text{–}^{15}N$ Correlations in Proteins

Timothy J. Norwood,* Jonathan Boyd, Nick Soffe, and Iain D. Campbell

Department of Biochemistry, University of Oxford South Parks Road, Oxford OX1 3QU, England

Received May 30, 1990

An exciting advance in the last few years has been the demonstration that complete structures of proteins in solution can be deduced from high-resolution NMR data. The use of inverse detection heteronuclear $^1H\text{–}^{15}N$ NMR techniques in conjunction with ^{15}N labeling has proved invaluable for such studies.[1-4] Experiments that reveal not only intraresidue correlations but also interresidue ones[5-9] between $C_\alpha H(i)$ and $^{15}N(i+1)$ are particularly useful since they aid sequential assignment.[10-15] In addition, the heteronuclear scalar coupling giving rise to a correlation between $C_\alpha H(i)$ and $^{15}N(i+1)$ is very sensitive to the backbone torsion angle, ψ, and is consequently a source of structural information;[11,12] for example, $J \simeq 6$ Hz for α-helical regions and $J < 1.5$ Hz in β-sheets. The HMBC (^1H-detected *h*eteronuclear *m*ultiple *b*ond *c*orrelation) experiment[5-9] has been successfully used to obtain this information, Figure 1A. There are however disadvantages to this experiment; for example, the data cannot be recorded in the pure absorption mode. Consequently spectra are usually displayed in mixed-mode absorption in F_1 and absolute-value mode in F_2. This hinders the recovery of the heteronuclear coupling constant.[9] Correlation peaks exhibit a homonuclear ^1H multiplet in F_1 that reduces the signal-to-noise ratio and increases the possibility of peak overlap. In this communication we propose a new technique that has a number of advantages over the HMBC experiment.

The alternative multiple bond pulse sequence described here (Figure 1B) allows data to be acquired in the pure absorption mode; all correlations that occur in the spectrum are singlets in F_1 and multiplets antiphase with respect to the active heteronuclear coupling in F_2. Consequently the heteronuclear coupling constant

(1) Marion, D.; Driscoll, P. C.; Kay, L. E.; Wingfield, P. T.; Bax, A.; Gronenborn, A. M.; Clore, G. M. *Biochemistry* **1989**, *28*, 6150.
(2) Kay, L. E.; Torchia, D. A.; Bax, A. *Biochemistry* **1989**, *28*, 8972.
(3) Montelione, G. T.; Winkler, M. E.; Rauenbuhler, P.; Wagner, G. *J. Magn. Reson.* **1989**, *82*, 198.
(4) Wider, G.; Neri, D.; Otting, G.; Wuthrich, K. *J. Magn. Reson.* **1989**, *85*, 426.
(5) Bax, A.; Summers, M. F. *J. Am. Chem. Soc.* **1986**, *108*, 2093.
(6) Bax, A.; Marion, D. *J. Magn. Reson.* **1988**, *78*, 186.
(7) Clore, G. M.; Bax, A.; Wingfield, P.; Gronenborn, A. M. *FEBS Lett.* **1988**, *238*, 17.
(8) Bax, A.; Sparks, S. W.; Torchia, D. A. *J. Am. Chem. Soc.* **1988**, *110*, 7926.
(9) Titman, J. J.; Neuhaus, D.; Keeler, J. *J. Magn. Reson.* **1989**, *85*, 111.
(10) Karplus, M. *J. Am. Chem. Soc.* **1963**, *85*, 2870.
(11) Bystrov, V. F. *Prog. Nucl. Magn. Reson. Spectrosc.* **1976**, *10*, 41.
(12) Schulz, G. E.; Schirmer, R. E. *Principles of Protein Structure*; Springer: Berlin, 1979.
(13) Cowburn, D.; Live, D. H.; Fischman, A. J. *J. Am. Chem. Soc.* **1983**, *105*, 7453.
(14) Fischman, A. J.; Live, D. H.; Wyssbrod, H. R.; Agosta, W. C.; Cowburn, D. J. *J. Am. Chem. Soc.* **1980**, *102*, 2533.
(15) Kessler, H.; Griesinger, C.; Wagner, K. *J. Am. Chem. Soc.* **1987**, *109*, 6927.

0002-7863/90/1512-9638$02.50/0

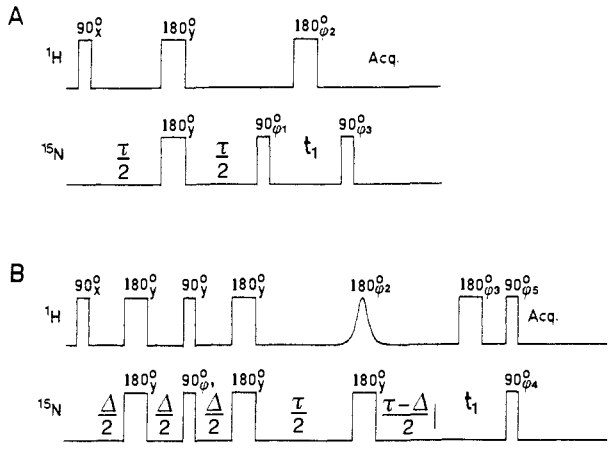

Figure 1. Pulse sequences for heteronuclear ^1H–^{15}N long range correlation spectroscopy. (A) HMBC experiment. (B) SQMBC experiment. $\Delta = (1/2^1J_{NH})$, and $\tau \simeq (1/4^mJ_{NH})$, where $^mJ_{NH}$ is the long range ^1H–^{15}N coupling constant. The fifth pulse of B is a complex hyperbolic secant shaped soft pulse calibrated to invert the region of the proton spectrum to which multiple bond correlations are to be observed. Phase cycling: for A, $\phi_1 = (x,-x)$, $\phi_2 = 2(x,y,-x,-y)$, $\phi_R = (x,-x) + 2(x,-x)$; for B, $\phi_1 = (x,-x)$, $\phi_2 = 2(x,y,-x,-y)$, $\phi_3 = 8(x,y,-x,-y)$, $\phi_4 = 32(x,-x) + 64(x,-x)$, $\phi_5 = 64(x,-x)$, $\phi_R = (x,-x) + 32(x,-x)$. The number before each bracketed phase cycle indicates the number of consecutive transients that are acquired with each step. When a phase expression is a linear combination of bracketed cycles, the phases calculated from each one are added together to obtain the phase to be used. Phase-sensitive data were acquired by incrementing the 90°(^{15}N) pulse subsequent to the t_1 period according to the States method.[20]

can be extracted more easily and the probability of peak overlap in the F_1 dimension is greatly reduced. While the HMBC experiment relies on the generation of heteronuclear ^1H–^{15}N multiple-quantum coherence to encode the ^{15}N chemical shift in the F_1 dimension of the spectrum, the experiment that we demonstrate here utilizes ^{15}N single-quantum coherence[16-18] for this purpose. To optimize sensitivity, the pulse sequence incorporates a soft pulse that is used to channel magnetization exclusively to the correlations of interest, in this case those between ^{15}N and the C_α protons. For brevity we call the experiment SQMBC: *s*ingle-*q*uantum *m*ultiple *b*ond *c*orrelation experiment.

In the HMBC experiment, Figure 1A, proton magnetization is initially generated, and this evolves during a subsequent proton evolution period τ due to its long-range heteronuclear ^1H–^{15}N scalar couplings. Those components of proton magnetization that have become antiphase with respect to heteronuclear couplings are then converted into heteronuclear multiple-quantum coherence. After an evolution period t_1, this is converted back into antiphase magnetization, which is detected as it becomes in-phase. The F_1 multiplets of peaks present in HMBC spectra arise from the fact that heteronuclear multiple-quantum coherence evolves due to the homonuclear scalar couplings of its active proton during the t_1 interval; the mixed phase results from the presence of both homonuclear ^1H and heteronuclear ^1H–^{15}N scalar coupling evolution during τ. In the SQMBC experiment, Figure 1, ^{15}N single-quantum coherence is generated from amide proton magnetization via the large mutual one-bond scalar coupling ($^1J_{NH}$). Since the generation period, Δ, required for this is relatively small ($\Delta = 1/(2^1J_{NH}) \simeq 5$ ms), homonuclear proton scalar coupling evolution can be neglected ($1/(2^3J_{HH}) \simeq 60$ ms). The subsequent period τ is designed so that, at its termination, a ^{15}N single-quantum coherence will be in-phase with respect to its one-bond heteronuclear coupling and antiphase with respect its long-range heteronuclear couplings to the protons of interest, the C_α protons. In the current study the soft pulse used to invert selectively the protons of interest was a complex hyperbolic secant.[19] This pulse

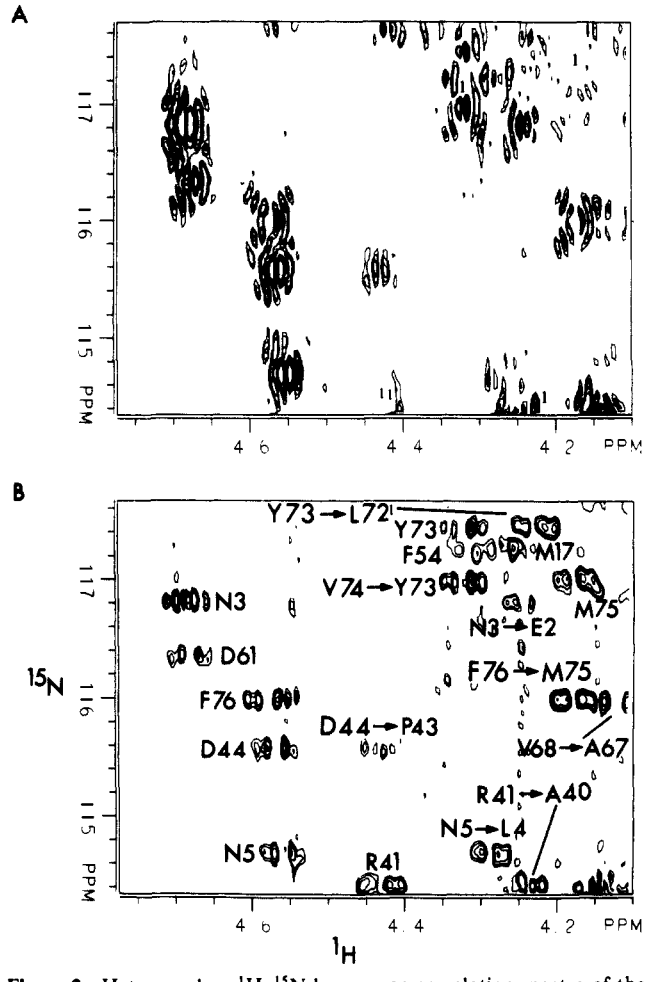

Figure 2. Heteronuclear ^1H–^{15}N long range correlation spectra of the c subunit of the ATP-synthase of *E. coli* (10 mM in trifluoroethanol-d_2) obtained with (A) the pulse sequence given in Figure 1A and (B) the pulse sequence given in Figure 1B. In each case $\Delta = 5.25$ ms, $\tau = 40$ ms for A and 50 ms for B, $F_1 = 1400$ Hz, and $F_2 = 6000$ Hz; 256 t_1 increments were acquired with 256 transients each. 90° pulse lengths were 7.2 μs for ^1H and 36.5 μs for ^{15}N. The 180°(^1H) soft pulse used for B was a 15-ms complex hyperbolic secant with[19] $\mu = 5$ and an effective inversion bandwidth of ±350 Hz centered on the α-protons. No solvent presaturation was used in either case. All experiments were performed on a spectrometer operated by a GE 1280 computer with an 11.8-T vertical-bore Oxford Instruments magnet operating at 500.1 MHz for ^1H and 50.7 MHz for ^{15}N.

shape was chosen because it inverts longitudinal magnetization efficiently over a well-defined region but has little effect outside it. The pulses subsequent to the t_1 period convert the ^{15}N coherence back into proton magnetization that is observed as it becomes in-phase. All peaks will be singlets in F_1 since no net scalar coupling evolution occurs during t_1. Since homonuclear proton scalar coupling evolution prior to data acquisition is minimal, F_2 multiplets will be pure absorption and only antiphase with respect to the active heteronuclear coupling.

Although the new experiment is longer by a period Δ than its HMBC counterpart, it will still usually exhibit a better overall signal-to-noise ratio, partly because the ^{15}N single-quantum coherence evolving during τ often decays at a slower rate than the proton magnetization evolving in the corresponding period of the HMBC experiment. Of course slower relaxation allows a longer value of τ to be used, thus increasing the efficiency of coherence transfer. An additional source for the improved signal-to-noise ratio of the new experiment lies in the fact that the intensity of a peak will no longer be spread out over a multiplet in the F_1

(16) Bodenhausen, G.; Ruben, D. J. *Chem. Phys. Lett.* **1980**, *69*, 185.
(17) Norwood, T. J.; Boyd, J.; Campbell, I. D. *FEBS Lett.* **1989**, *255*, 369.
(18) Norwood, T. J.; Boyd, J.; Heritage, J.; Soffe, N.; Campbell, I. D. *J. Magn. Reson.* **1990**, *87*, 488.
(19) Silver, M. S.; Joseph, R. I.; Hoult, D. I. *Phys. Rev.* **1985**, *A31*, 2753.
(20) States, D. J.; Haberkorn, R. A.; Ruben, D. J. *J. Magn. Reson.* **1982**, *48*, 286.

dimension. Furthermore, SQMBC line widths are narrower in F_1 than their HMBC counterparts since the line width of a heteronuclear multiple-quantum coherence giving rise to a multiple bond correlation will effectively be equal to the sum of the linewidths of its active spins; although mutual dipolar relaxation vanishes in the slow tumbling limit, this will not be the major source of relaxation for either spin. Since the SQMBC experiment relies on the initial generation of amide proton magnetization, the experiment must be performed in H_2O; for the same reason presaturation will not eliminate correlations to spins underneath the solvent signal. Another possible disadvantage is that the greater number of pulses in the SQMBC experiment will make it more difficult to obtain artifact-free spectra.

The two experiments are demonstrated and compared in Figure 2 on a uniformly ^{15}N labeled sample of the 79-residue c subunit of the ATP-synthase of *Escherichia coli*. In the case of the SQMBC experiment, the soft pulse was set up to invert the α-protons, thus channeling coherence to this region of the spectrum. The SQMBC spectrum is clearly superior since its peaks are better resolved and are pure absorption; it also exhibits a much more uniform distribution of intensity among peaks, although some individual HMBC peaks are more intense than their SQMBC counterparts. It should be noted that since the SQMBC experiment incorporates more pulses than HMBC, it will be more sensitive to rf inhomogeneity and pulse miss-setting. Although correlations to the C_α protons were chosen for the current study, others, for example, β-protons, could have been chosen as easily.

Acknowledgment. We thank Jane Heritage for preparing the c-subunit sample. This is a contribution from the Oxford Centre for Molecular Sciences and was supported by the SERC and the MRC.

Registry No. ATP synthase, 37205-63-3.

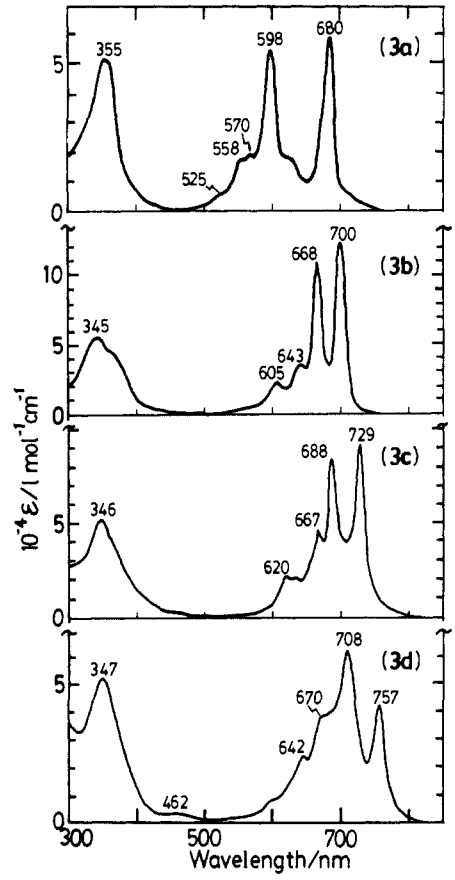

Figure 1. UV-visible-near IR absorption spectra of **3a-d** in *o*-dichlorobenzene.

New Route to Unsymmetrical Phthalocyanine Analogues by the Use of Structurally Distorted Subphthalocyanines

Nagao Kobayashi,* Ryoko Kondo, Shin-ichiro Nakajima, and Tetsuo Osa*

Pharmaceutical Institute, Tohoku University Aobayama, Aoba, Sendai 980, Japan

Received September 17, 1990

In addition to traditional uses as dyes and in photocopying devices,[1] phthalocyanines (Pcs) are now rapidly growing in importance in many fields such as chemical sensors, electrochromism, batteries, photodynamic cancer therapy, molecular metals, photochemical hole burning, and liquid crystals.[2] Although symmetrical tetra-, octa-, and hexadecasubstituted Pcs are well documented, there have been few reports on Pc analogues with lower symmetry mainly because of their preparative difficulty. These compounds are also important in applications and in understanding the nature of Pcs. For example, fine tuning of the position of the absorption band of Pcs can be achieved by the stepwise introduction of peripheral substituent groups[3] or by the stepwise adjustment of the size of the π-conjugated macrocyclic systems. Strategies of synthesis, based on using statistical condensation reactions of two different *ortho* dinitriles of aromatic compounds, give mixtures of products[4a] that cannot be readily separated by chromatographic methods, although a polymer support method can be used.[4b] In this communication, we present a completely new method for the preparation of monosubstituted type unsymmetrical Pcs and Pc analogues, which utilizes the so-called subphthalocyanines (SubPcs).[5]

Scheme I

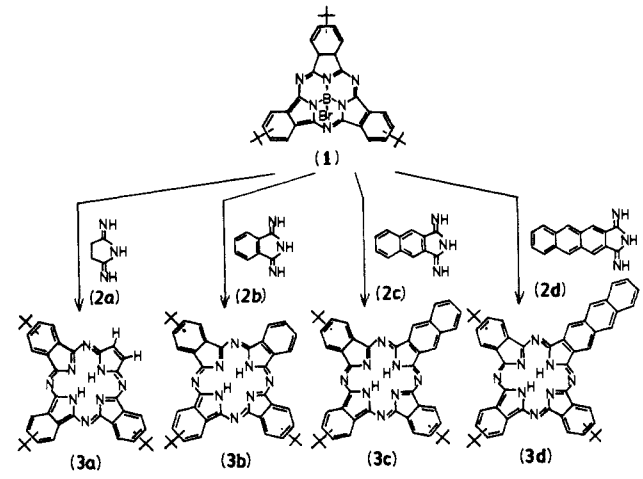

(1) Moser, F. H.; Thomas, A. H. *The Phthalocyanines*; CRC Press: Boca Raton, FL, 1983; Vols. I and II. Lever A. B. P. *Adv. Inorg. Chem. Radiochem.* **1965**, *7*, 27-114.

(2) (a) Lever, A. B. P.; Hempstead, M. R.; Leznoff, C. C.; Lin, W.; Melnik, M.; Nevin, W. A.; Seymour, P. *Pure Appl. Chem.* **1986**, *58*, 1467-1476. (b) Lever, A. B. P. *CHEMTECH* **1987**, 506-510. (c) Collins, R. A.; Mohammed, K. A. *J. Phys.* **1988**, *D21*, 154-161. (d) Spikes, J. D. *Photochem Photobiol.* **1986**, *43*, 691-699. (e) Snow, A. W.; Jarvis, N. L. *J. Am. Chem. Soc.* **1984**, *106*, 4706-4711. (f) Wohrle, D. *Adv. Polym. Sci.* **1983**, *50*, 45-134. (g) Simon, J.; Sirlin, C. *Pure Appl. Chem.* **1989**, *61*, 1625-1629. (h) Shutt, J. D.; Batzel, D. A.; Sudiwala, R. V.; Rickert, S. E.; Kenney, M. E. *Langmuir* **1988**, *4*, 1240-1247. (i) Piechocki, C.; Simon, J.; Skoulios, A.; Guillon, D.; Weber, P. *J. Am. Chem. Soc.* **1982**, *104*, 5245-5247.

(3) (a) Stillman, M. J.; Nyokong, T. In *Phthalocyanines-Properties and Applications*; Leznoff, C. C., Lever, A. B. P., Eds.; VCH: New York, 1989; Chapter 3. (b) Konami, H.; Hatano, M. *Chem. Lett.* **1988**, 1359-1362.

(4) (a) Piechocki, C.; Simon, J. *J. Chem. Soc., Chem. Commun.* **1985**, 259-260. (b) Leznoff, C. C. In *Phthahlocyanines-Properties and Applications*; Leznoff, C. C., Lever, A. B. P., Eds.; VCH: New York, 1989; Chapter 1.

0002-7863/90/1512-9640$02.50/0